PROC. 19th INT. CONF. HIGH ENERGY PHYSICS
TOKYO, 1978

P 7b

Neutrino Interactions II: Neutral Current Interactions and Charm Production

C. BALTAY

Columbia University, New York, NY. 10027

§1. Introduction

In the usual current-current theory of the weak and electromagnetic interactions, the interactions can be classified as:

a. The electromagnetic current, such as (e~, e⁺), (/?, *p),* (7T⁺, 7T~), etc., which is responsible for the electromagnetic interactions. The properties of this current are that it is charge conserving *(dQ=0),* has a pure vector spatial structure *(V),* and has isospin *1=0* and 1 parts.

b. The weak charged current, such as (e~, ***v),*** (//", (n, ***p),*** etc., which is responsible for the weak decay processes and the first neutrino interactions that were observed. This current is charge chaning (Jg=l), has a V-A structure, and is isospin /= 1.

c. The weak neutral currents, such as (e~, e⁺), (y, v), (/?, *p),* etc. This is a charge conserving *(JQ=0)* or "neutral" current. Its spatial (V, A, S, P, T?) and isospin (/=?) structure is the subject of a large portion of this talk.

Until 1971-72, the weak neutral currents were widely believed to be absent in nature, in part due to the low experimental limits on various processes such as K± -> 7r± + e⁺ + e~ or K£-> //⁺+//~, or *vp—^vp.* However, in 1973-74 weak neutral currents were discovered experimentally in elastic neutrino interactions[1] and in single pion production processes by neutrinos.[2] In the past four years, a great deal of data on neutral currents has been accumulated, so that for the first time at this Conference, we can say that the main features of the neutral current interactions are understood.

The discovery of neutral currents was strongly motivated by the Weinberg-Salam model[3] (W-S), and this model together with the Glashow-Iliopoulos-Maiani[4] (G-I-M) charm scheme gives an adequate description of all of the experimental data. In §11. A of the talk, the survey of the experimental situation, the experimental results will be compared with the prediction of the W-S model. In §11. B, the determination of the neutral current couplings, a "model independent" analysis will be followed, not assuming any specific model but using the experimental data to determine the relevant neutral current couplings. As we will see, the couplings obtained are just those of the W-S model.

In order to be able to discuss the predictions of the W-S model meaningfully, and introduce the terminology, we give here a very brief outline of some features of the model. The model introduces, among other things, four intermediate vector bosons:

Isotriplet	W^+	W^0	W^-
Isosinglet		B^0	

The neutral members of these bosons mix to give the physical Z° and the r:

$$Z^0 = \cos\theta W^0 + \sin\theta B^0$$
$$\gamma = -\sin\theta W^0 + \cos\theta B^0,$$

where *0* is a mixing angle (the Weinberg angle) to be determined by experiments. The $W^\pm$ mediate the usual charged current weak interactions, the Z° mediates the neutral current weak interactions, and the *y* mediates the electromagnetic interactions.

The mixing angle can be expressed in terms of the coupling constants of the intermediate vector bosons to leptons:

g —coupling constant of isotriplet to leptons,
g'—coupling constant of isosinglet to letpons.

In terms of these coupling constants,

$$\sin\theta = \frac{g'}{\sqrt{g^2+g'^2}} \; ; \; \cos\theta = \frac{g}{\sqrt{g^2+g'^2}}.$$

The electromagnetic coupling constant is

$$e = \frac{gg'}{\sqrt{g^2+g'^2}},$$

and the ratio of the electromagnetic to the weak coupling constants is

$$e^2/g^2 = \sin^2\theta$$

The Fermi coupling constant *G* can be ex-

pressed in terms of the above coupling constants and the intermediate boson mass, M_w, as

$$G=\frac{\sqrt{2}g^2}{8M_{W\pm}^2}$$

or

$$M_{W\pm}^2=\frac{\sqrt{2}g^2}{8G}=\frac{\sqrt{2}e^2}{8G\sin^2\theta}$$

and similarly for the Z°:

$$M_{Z0}^2=\frac{\sqrt{2}(g^2+g'^2)}{8G}=\frac{M_{W\pm}^2}{\cos^2\theta}.$$

Thus the masses of the intermediate bosons are given in terms of the known constants e and G and the single free parameter of the model, $\sin^2\theta$. For values of $\sin^2\theta$ near 1/4, the masses are predicted to be

$$M_{W\pm}\sim 75\ \text{GeV}$$
$$M_{Z0}\sim 90\ \text{GeV}.$$

This model predicted the existence of weak neutral currents. However, experimentally strangeness changing neutral currents were known to be absent in K decays. This motivated the G-I-M mechanism, in which a new hadronic quantum number, charm, was introduced to cancel out the strangeness changing neutral currents, while allowing strangeness conserving neutral currents. In quark language, this implies the introduction of a fourth quark to the still undiscovered triplet of quarks, as follows

Quark	Charge	Strangeness	Charm
u	+2/3	0	0
d	−1/3	0	0
s	−1/3	−1	0
c	+2/3	0	1

In order for this cancellation to work, the couplings between the quarks in terms of the Cabibbo angle must be

z/-+cos $0_c(d+\wedge^+)$+sin $6_c(s+W^+)$
c-+sin $0_c(d+W^+)$+cos $d_c(s+W^+)$.

The G-I-M charm scheme also predicetd the existence of a new family of charmed hadrons. This seemed to be a problem until just recently when charmed particles were indeed found experimentally. Note that the above coupling scheme implies that charmed particles will decay predominantly into strange particles.

In the W-S model, the cross sections and other properties of the weak neutral current processes are determined in terms of the single free parameter, $\sin^2 0$, For example, in the purely leptonic neutrino-electron scattering processes

$$\nu+e^-\to\nu+e^-,$$

the differential cross section is given by

$$\frac{d\sigma}{dy}=\frac{G^2m_eE_\nu}{2\pi}[(g_V+g_A)^2+(g_V-g_A)^2(1-y)^2],$$

where $y=E_e/E_\nu$, the ratio of the energy of the final state electron to the incident neutrino energy. The constants g_v and g_A are, for the four processes:

Process	V–A Theory		Weinberg–Salam	
	g_V	g_A	g_V	g_A
$\nu_e+e^-\to\nu_e+e^-$	1	+1	$1/2+2\sin^2\theta$	+1/2
$\bar\nu_e+e^-\to\bar\nu_e+e^-$	1	−1	$1/2+2\sin^2\theta$	−1/2
$\nu_\mu+e^-\to\nu_\mu+e^-$	0	0	$-1/2+2\sin^2\theta$	−1/2
$\bar\nu_\mu+e^-\to\bar\nu_\mu+e^-$	0	0	$-1/2+2\sin^2\theta$	+1/2

Thus the purely leptonic processes are completely determined in terms of the single parameter, $\sin^2$ and a theoretically unambiguous interpretation of the experiments is possible. For processes involving hadrons, however, uncertainties of varying degrees creep in due to hadronic form factors and other poorly understood features of hadronic interactions.

§11. Neutral Current Interactions

A. Summary of the experimental situation

Table I summarizes briefly the neutral current processes that have been experimentally studied with some comment on the difficulty of the theoretical interpretation. Unfortunately the theoretically cleanest processes are the most difficult to study experimentally because of their very low cross sections.

We now proceed to a discussion of the experimental status of the processes listed in Table I.

1. Purely leptonic processes

i. The process, $v_e+e"\to v_e+e\sim$, has been detected by Reines *et al.*[5] in an experiment at the Savannah River Fission Reactor using v_e with energies between 1 and 8 MeV. They obtained a result of

$$o(y_e+e\wedge v_e+\text{€})=(\backslash.06\pm 0.22)\quad_x\quad a_{v\text{-}A}$$

where G_v~A is the cross section predicted for this process by the V-A theory, 0.54×10^{-41}

Table I. Experimentally studied N. C. processes.

Process	Comparison with theory
1. Purely leptonic	
$\nu_\mu + e^- \to \nu_\mu + e^-$	Very clean
$\bar{\nu}_\mu + e^- \to \bar{\nu}_\mu + e^-$	(No hadrons involved)
$\bar{\nu}_e + e^- \to \bar{\nu}_e + e^-$	
2. Elastic scattering	Relatively straightforward.
$\nu_\mu + p \to \nu_\mu + \pi$	Some uncertainty due to
$\bar{\nu}_\mu + p \to \bar{\nu}_\mu + \pi$	proton form factors (M_A).
3. Single pion production	Model dependent due to
$\nu_\mu + N \to \nu_\mu + N' + \pi$	hadronic vertex.
$\bar{\nu}_\mu + N \to \bar{\nu}_\mu + N' + \pi$	Also nuclear physics corr.
4. Inclusive	Quark-parton model
$\nu_\mu + N \to \nu_\mu + \ldots$	Dependent.
$\bar{\nu}_\mu + N \to \bar{\nu}_\mu + \ldots$	
5. Atomic physics	Large uncertainites due to
$e^- + Bi \to e^- + Bi$	atomic physics calculations.
6. Electron scattering	Quark–parton model
$\vec{e}^- + d \to e^- + \ldots$	dependent.

E_ν cm²/GeV. This process can proceed by either the standard charged current V-A interaction or by neutral currents. The theoretically predicted cross section for both the V-A interactions and the W-S model of the weak neutral currents, with the experimental detection efficiency folded in, is shown on Fig. 1 as a function of $\sin^2 \theta$. The experimental

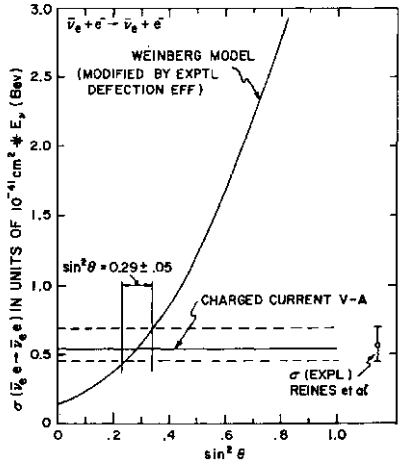

Fig. 1. Comparison of the experimental result on <j(v,+e~-»£+e-) with the prediction of the W-S model.

result is in agreement with either the V-A theory or with the W-S model with

$$\sin^2 0\text{-}O.29 \pm O.O5.$$

At this value of sin² #, the total cross section for this process is very similar for the V-A theory and the Weinberg-Salam model. However the distribution in the electron

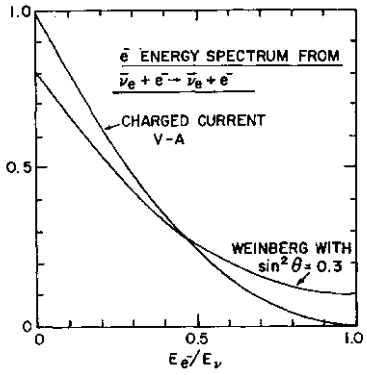

Fig. 2. Distribution in E_e/E_ν for the process v,+ e"->£,+e" in the charged current V-A theory and the W-S model.

energy E_e- is not the same in the two models, as shown in Fig. 2. The cross section for the W-S model is smaller than the V-A theory below $E_e\text{-}IE_\nu \sim \backslash j2$ and larger above.

The experimental cross sections when divided into low and high E_e- regions are

$\wedge ex,t=(0.85\pm0.25)X(7\wedge,\ 1.5<£_e\_<3.0MeV$

$\wedge pt=(l\text{-}70\_h0.44)xir_{F\_11},\ 3.0<£_e\text{-}<4.5MeV.$

This favors the W-S model, but the statistical significance is not conclusive.

ii. The experimental results on the process i^+e'-n^+e" are summarized in Table II. In the low energy Gargamelle experiment[6] at the CERN PS, one candidate for this reaction was observed with a background of 0.3±0.1 events. The signal was not considered significant and an upper limit for the cross section was quoted. In the low energy Aachen-Padova spark chamber experiment[7] at the CERN PS, 32 events were seen with a rather large background estimated to be 21 events. The high energy Gargamelle experiment[7] at the CERN SPS published[8] a result for the cross section that was about five times larger than the prediction of the W-S model,

$$(7.3\pm i{:}\text{»})x\ 10^{"42}£_\nu\ \text{cm}^2 < tf < (8.2\pm!;^7)$$
$$X10^{-42}£_\nu\ \text{cm}^2,$$

based on 10 observed events in a sample of 24,000 charged current interactions. Soon thereafter a Columbia-Brookhaven experiment at Fermilab using the 15 ft bubble chamber filled with heavy neon published** a result of

$$\wedge e\text{-}\text{-}>\wedge\text{-})\text{-}(1.8\pm0.8)x10^{-42}£',\text{cm}^2$$

based on 11 events found in a sample of

Table II. y^+e'-^+e .

Experiment	Total sample of $\nu_\mu + N \to \mu^- + \ldots$	Events observed	Background	Cross section 10^{-42} E_ν cm^2
Gargamelle[6] CERN PS		— 1	0.3±0.1	—3
Aachen–Padova[7] CERN PS spark Chamber		32	21	1.1±0.6
Gargamelle[8] CERN SPS	41,000	9	0.4±0.4	3.7+2.0 to 4.2+2.2 −1.3 −1.7
Columbia–NNL[9] Fermilab 15 ft chamber	160,000	11	0.7±0.7	1.8±0.8
Average				1.7±0.5

106,000 charged current interactions, not confirming the Gargamelle result, and in good agreement with the Weinberg-Salam model. At this conference the Gargamelle group reported a more recent value for the cross section of

$$(3.7^{+2.0}_{-1.5}) \times 10^{-42}\ E_\nu\ \text{cm}^2 \leq \sigma \leq (4.2^{+2.2}_{-1.7}) \times 10^{-42}\ E_\nu\ \text{cm}^2,$$

based on a scan of 75% more film with a combined 9 events in 41,000 charged current interactions. The agreement between the experiments shown on Table II, while not excellent, is no longer all that bad. The average of all the experiments is

$$\sigma(\nu_\mu + e^- \to \nu_\mu + e^-) = (1.7 \pm 0.5) \times 10^{-42} E_\nu\ \text{cm}^2$$

where the average is obtained by adding the numbers of events observed in the experiments and dividing by the sum of the effective denominators.

The signal for this reaction in the high energy bubble chamber experiments is very clean. Figure 3 shows the plot of θ_{e^-} the lab angle of the recoil electron, *vs* E_{e^-}, its lab energy, for the 11 Columbia-BNL events. All of the events are consistent with the kinematics of the reaction, i^+e~->iv+e~, shown by the curves on Fig. 3. A nice variable to show this is $E\theta^2$; the kinematic limit for this reaction is $E\theta^2 < 2\ m_e$, where m_e is the mass of

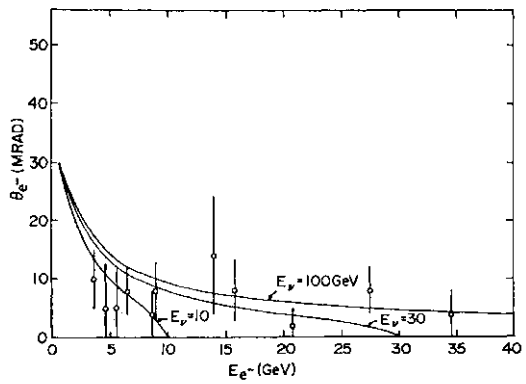

Fig. 3. Electron angle θ_{e^-} *vs* electron energy E_{e^-} for the 11 *Vfi+Q~->vfi+C* events (from ref. 9).

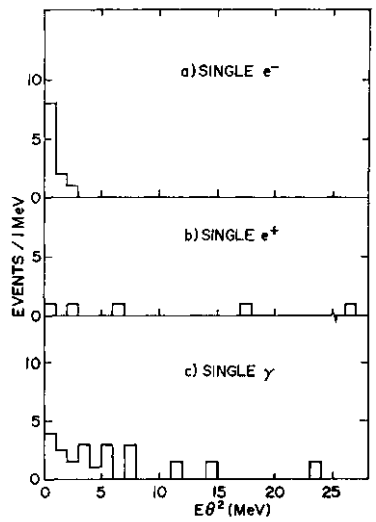

Fig. 4. Distribution in $E\theta^2_e$ for a) the single e~ events; b) the single e+ events and c) the single r->e++e~ events (from ref. 9).

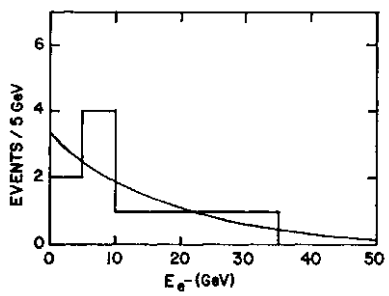

Fig. 5. Distribution in the electron energy E_e for the 11 *i>ti+s~-*vti+G~* events (from ref. 9). The curve is the prediction of the W-S model for $\sin^2 \theta = 1/4$.

the target electron. Figure 4 shows the distribution in this variable. The single e~ events peak below 1 MeV with a small tail above 1 MeV consistent with the experimental resolution. The single e^+ events, which are consistent with coming from the reaction $\nu_e + p \to e^+ + n$, and the single *j* events, are much more spread out in *E0\~,* as expected. The distribution in the electron energy E_{e^-} shown in Fig. 5, is consistent with the distribution predicted by the W-S model with $\sin^2 \theta \sim 1/4$, as shown by the curve on the figure.

The W-S model, with $\sin^2 \theta = 0.23$, predicts a cross section for this process of $<r = 1.5 \times 10^{-42}$ £, cm^2. The average value of 1.7±0.5 for all of the experiments is in good agreement with this prediction. Conversely the average value can be used to obtain a mixing angle of

$$\sin^2 \theta = 0.21 \pm ^{\circ};^{\circ}.$$

There is also a solution at a large value of $\sin^2 \theta$ as shown on Fig. 6a.

iii. The experimental results on the reaction $\nu + e^- \to \nu + e^-$ are summarized in Table III. All five experiments find results which are consistent with the W-S model which predicts a cross section of $\sigma = 1.3 \times 10^{-42} E_\nu$ cm^2 for this process for $\sin^2 \theta = 0.23$. The average of the two low energy experiments, where a signal is seen, is

$$(j(\nu + e^- \to \nu_{\mu} + e^-) = (1.8 \pm 0.9) \times 10^{-42} E_\nu \text{ cm}^2.$$

This value corresponds to a mixing angle of

$$\sin^2 \theta = 0.3111$$

in the W-S model, as shown on Fig. 6b.

2. Elastic scattering on protons

The process, $\nu + p \to \nu + p$, has been observed in four experiments, and $\bar{\nu} + p \to \bar{\nu} + p$ in one experiment, as listed in Table IV. The agreement between the experiments is good. The errors on the weighted averages shown on

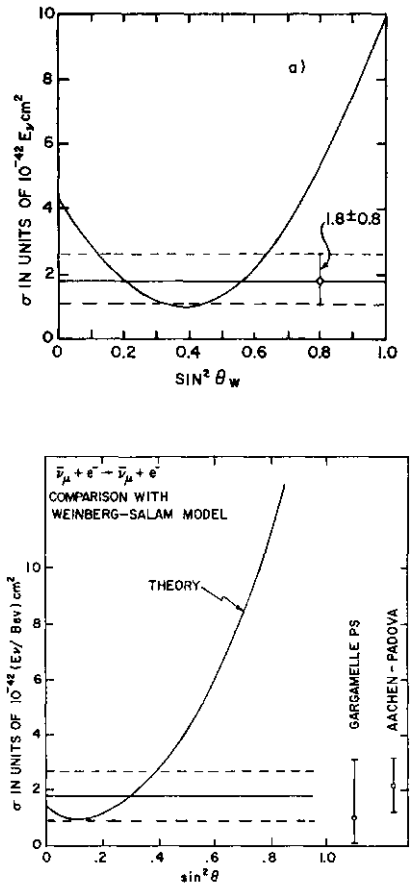

Fig. 6. Comparison of the experimental cross sections with the predictions of the W-S model for a) the reaction $\nu + e^- \to \nu + e^-$, and b) the reaction $\nu/<+e^- \to \nu + e^-$.

Table IV have increased by $\sqrt{2}$ since the quoted errors in the experiments are statistical only. The agreement between the averaged ratios and the W-S model is good, as shown on Fig. 7. The best value of the mixing angle from the reaction is

$$\sin^2 \theta = 0.26 \pm 0.06.$$

The q_h distribution for both the and scattering from the HPB experiment are shown in Fig, 8. Again the agreement with

Table III. $\nu + e^- \to \nu + e^-$.

Experiment	$\bar{\nu}_\mu + N \to \mu^+ + \ldots$	Events observed	Background	Cross section $10^{-42} E_\nu$ cm^2
Gargamelle[10] CERN PS		3	0.4±0.1	$1.0^{+2.1}_{-0.9}$
Aachen–Padova[11] CERN PS spark chamber		17	7.4±1.0	2.2±1.0
BEBC Wideband neon[12] CERN SPS	7,500	— 1	0.4±0.2	—3.5
Fermi–Mich–IHEP–ITEP[13] Fermilab 15 ft neon	6,300	0		—2.9
Gargamelle[14] CERN SPS	4,000	0		—3.3

Table IV. Elastic scattering on protons.

Experiment	$\nu_\mu+p\to\nu_\mu+p$			$\bar{\nu}_\mu+p\to\bar{\nu}_\mu+p$		
	Events observed	Back-ground	$\frac{\nu_\mu+p\to\nu_\mu+p}{\nu_\mu+n\to\mu^-+p}$	Events observed	Back-ground	$\frac{\nu_\mu+p\to\nu_\mu+p}{\bar{\nu}_\mu+p\to\mu^++n}$
Harvard–Penn–BNL[15] BNL counter detector	255	88	0.11 ± 0.02	69	28	0.19 ± 0.05
Columbia–Ill–Rock[16] BNL spark chamber	71	30	0.20 ± 0.06			
Aachen–Padova[17] CERN PS S.C.	155	110	0.10 ± 0.03			
Gargamelle[18] CERN PS	100	62	0.12 ± 0.06			
Weighted average*,†			0.11 ± 0.02			0.19 ± 0.08

* Errors increased by V 2 since quoted errors statistical only.

† Caution—the experiments have slightly different Q^2 cuts.

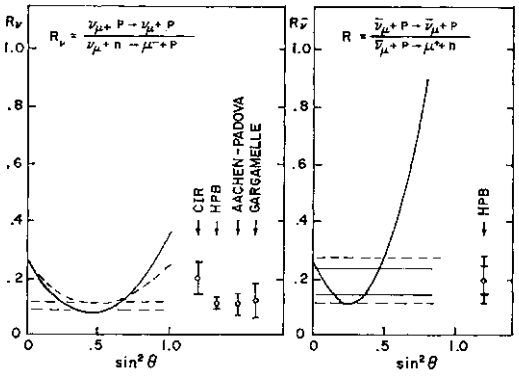

Fig. 7. Comparison of the experimental cross section ratios with the predictions of the W-S model for a) the reaction yju + p - ^ + P and b) the reaction i^ + p - ^ + p .

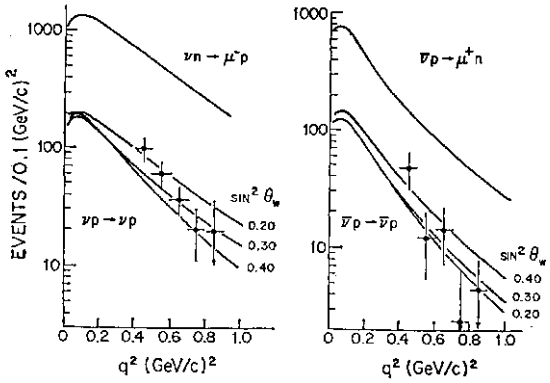

Fig. 8. Distribution in q^2, compared with the predictions of the W-S model for various values of $\sin^2\theta$, for a) yju + p - ^ + p and b) i^ + p - ^ + p (from ref. 15).

the predictions of the W-S model, shown by the curves on the figure, is good with values of sin² 0-1/4.

3. *Single pion production*

The large amount of data that is available on the various neutral current single pion production processes is summarized in Table V. The predictions of the W-S model for these reactions, listed in the last column on the table, are model dependent because of the form factors at the hadronic vertex. The model developed by Adler[23] is the basis for the numbers given in the table. The theoretical uncertainty on these is substantial, as indicated by the errors given on some of the numbers. There is an additional uncertainty on the ratios measured using complex nuclear targets due to the rescattering of the final state pion. In view of these uncertainties, the agreement between the experimental results and the model is satisfactory, as can be seen from a comparison of the last two columns on Table V.

The pion-nucleon mass distribution in the neutral current single pion production processes indicates that the J(1238), the 7=3/2 pi-nucleon resonance is produced in these reactions. Figure 9 shows the prc° and the p:r~ mass distributions in the reactions J^ + p - ^ + p + Tr° and i^ + n - ^ + p + Tr"-, respectively, in the Gargamelle propane experiment. This is significant because it shows in a model independent way that the neutral current is not pure isoscalar but has a sizeable isovector part to transform an 7=1/2 nucléon into an 7=3/2 J(1238). This conclusion is important in resolving the isoscalar-isovector ambiguity in the model independent analysis of the neutral current couplings.

4. *Inclusive reactions*

The neutral to charged current ratios for both ***Va*** and v« induced inclusive reactions

$$R_\nu=\frac{\nu_\mu+X\to\nu_\mu+\cdots}{\nu_\mu+X\to\mu^-+\cdots}$$

$$R_\nu=\frac{\bar{\nu}_\mu+X\to\bar{\nu}_\mu+\cdots}{\bar{\nu}_\mu+X\to\mu^++\cdots}$$

Table V. Single pion production.

Experiments	Ratio measured	Exptl. result	W-S $\sin^2\theta \sim 1/4$[22]
CIR[19] Aachen–Padova	$\{(\nu+X+\pi^0)\}/\{2(\mu^-+X+\pi^0)\}$	0.21 ± 0.07*	$0.24\pm$
Gargamelle complex nuclei	$\{(\bar{\nu}+X+\pi^0)\}/\{2(\mu^++X+\pi^0)\}$	0.46 ± 0.10*	$0.30\pm$
Argone[20]	$\{\nu+n+\pi^+\}/\{\mu^-+p+\pi^+\}$	0.13 ± 0.06	$0.07\pm$
12 ft B.C.	$\{\nu+p+\pi^0\}/\{\mu^-+p+\pi^+\}$	0.40 ± 0.22	$0.17\pm$
deuterium	$\{\nu+p+\pi^-\}/\{\mu^-+p+\pi^+\}$	0.12 ± 0.04	$0.07\pm$
Gargamelle[21]	$\{(\nu p\pi^0)+(\nu n\pi^0)\}/\{2(\mu^-+p\pi^0)\}$	0.45 ± 0.08	$0.42\pm$
CERN PS	$\{(\bar{\nu}p^0)+(\bar{\nu}n\pi^0)\}/\{2(\mu^+n\pi^0)\}$	0.57 ± 0.11	$0.60\pm$
propane	$\{\nu+p+\pi^0\}/\{\mu^-+p+\pi^0\}$	0.56 ± 0.10	0.42 ± 0.13
	$\{\nu+n+\pi^0\}/\{\mu^-+p+\pi^0\}$	0.34 ± 0.09	0.42 ± 0.13
	$\{\nu+p+\pi^0\}/\{\mu^-+p+\pi^0\}$	0.45 ± 0.13	0.28 ± 0.08
	$\{\nu+n+\pi^+\}/\{\mu^-+p+\pi^0\}$	0.34 ± 0.07	0.28 ± 0.08

* Weighted average of three experiments. Agreement between experiments not very good. Errors caled by $\sqrt{\chi^2/n-1}$. Average may not be valid ! !

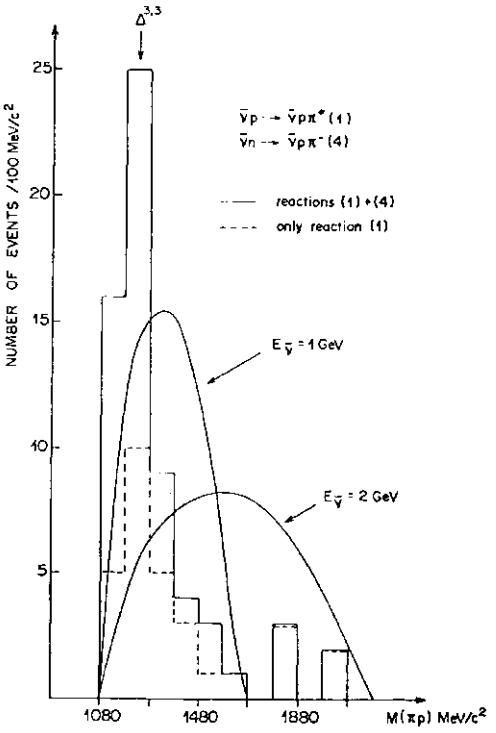

Fig. 9. Nucleon-pion mass distributions from the reactions v+p->£+P+rc° and v+n-*£+p+7r~ (from ref. 21).

have been measured in a large number of experiments. Their results are summarized in Table VI. The targets *(x)* used were mostly heavy nuclei, so that the ratios are averages for approximately equal number of neutrons and protons. A cut on the visible hadronic energy has been used in all of the experiments. The raw ratios with the E_h cuts are listed in the table. The last two columns give the ratios extrapolated to $E_h=0$. The agreement between the experiments is very good, especially when one considers that the incident neutrino energies vary from a few GeV to a few hundred GeV in the various experiments. The measured ratios are also in good agreement with the predictions of the W-S model, as shown in Fig. 10. The weighted averages for the ratios are

$$£,=0.29=1=0.01$$

$$\wedge=0.35=1:0.025.$$

The ratio R_u implies a value of the mixing angle of

$$\sin^2\theta=0.24\pm0.02.$$

The determination of $\sin^2 6$ from R_v is somewhat dependent on quark-parton model assumptions. However, the current understanding of the quark parton model is such that these uncertainities are not very large, and are estimated to be comparable to the quoted error on $\sin^2 6$ of ±0.02. Paschos and Wolf en stein[31] have pointed out that the quark-parton model dependence cancels out in the ratio

$$R=\frac{\sigma^{\nu}_{NC}-\sigma^{\bar{\nu}}_{NC}}{\sigma^{\nu}_{CC}-\sigma^{\bar{\nu}}_{CC}}=1/2-\sin^2\theta.$$

Using this method the BEBC narrow band experiment obtained[32]

$$\sin^2\theta=0.22\pm0.05.$$

5. *Parity violation in atomic bismuth*

Due to the weak neutral current interaction between an atomic electron and the nucleus, parity violating effects at the 10^{-7} level might

Table VI. Inclusive neutral current ratios.

Experiment	E_ν GeV	E_h cut GeV	$R_\nu=\nu_\mu+N\to\nu_\mu+\cdots/\nu_\mu+N\to\mu+\cdots$ Raw Ratios R_ν	$R_{\bar\nu}$	R_ν Corrected for E_h Cut	$R_{\bar\nu}$
Gargamelle[24] CERN PS	1–10	1	0.25±0.04	0.56±0.08	0.26±0.04	0.39±0.06
HPWF[25] Fermilab	30–200	4	0.28±0.03	0.39±0.10	0.30±0.04	0.33±0.09
CITF[26] Fermilab	30–200	12	0.28±0.03	0.35±0.11	0.27±0.02	0.40±0.08
CDHS[27] CERN SPS	30–200	12	0.29±0.01	0.35±0.03	0.295±0.01	0.34±0.03
BNL 7 ft B.C.[28] deuterium	1–10	0.4	0.25±0.05			
BEBC Narrowband[29] CERN SPS neon	30–200	15	0.32±0.03	0.39±0.07	0.31±0.04	0.37±0.08
Mariner *et al.*[30] Fermilab 15 ft neon	10–100	10	0.35±0.06			
Weighted average					0.29±0.01	0.35±0.025

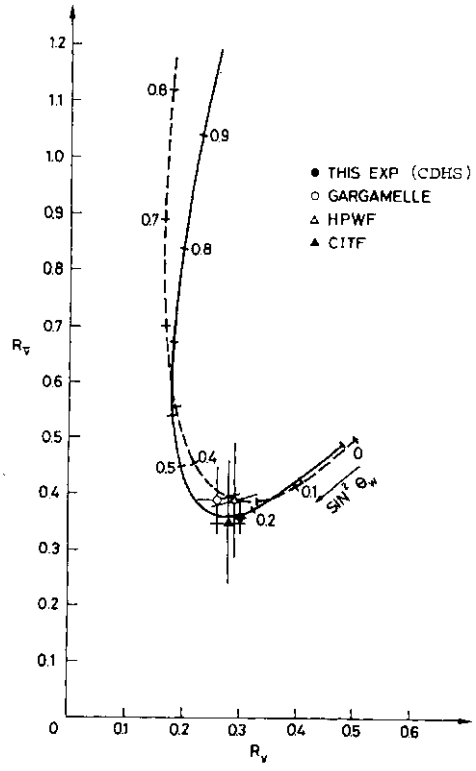

Fig. 10. Comparison of the experimental cross section ratios R_ν and $R_{\bar\nu}$ for the inclusive neutral current processes with the predictions of the W-S model with no antiquark contributions (dashed curve) and with the best estimate of the antiquark contribution, $q/q=0.1$ (solid curve), from ref. 27.

be expected m heavy nuclei like Bismuth 209. The effect is due to the V-A interference term between the vector part of the hadronic current and the axial vector part of the leptonic neutral current. The experiments measure the optical rotation of the plane of polarization of incident plane polarized laser light. A nonzero rotation measures a preferred direction (clockwise or counterclockwise) and is thus clearly parity violating. The results obtained in three experiments are summarized in Table VII. The agreement between the experiments is very poor. The predictions of the W-S model, listed in the last column of Table VII, have very large uncertainties due to the complex atomic physics calculations involved.[36] Bismuth has 83 atomic electrons, 3 valence and 80 in the core. The effects of the 80 core electrons are apparently very difficult to calculate. In view of these theoretical uncertainties and the disagreement between the three experiments, no conclusion seems warranted at this time, and one should not be too concerned about any possible discrepancies with the W-S model.

Table VII. Optical rotation in atomic bismuch.

Experiment	Transition Used	Observed optical rotation, $\times10^{-8}$	Weinberg–Salam prediction, $\times10^{-8}$
Seattle[33]	8757 Å	−0.5±1.7	−10 to −18
Oxford[34]	6480 Å	−5 ±1.6	−13 to −23
Novosibirsk[35]	6480 Å	−19 ±5	−13 to −23

6. Parity violation in polarized electron scattering

Interference between the weak neutral current and the electromagnetic interactions can lead to parity violating effects in polarized electron scattering

$$e^- \text{ (polarized)} + d \to e^- + \cdots$$

An experiment to look for such effects has been carried out at SLAC.[37] The experiment measured the asymmetry between the cross sections of left and right handed polarized incident electrons

$$A=\frac{\sigma(\overleftarrow{e})-\sigma(\overrightarrow{e})}{\sigma(\overleftarrow{e})+\sigma(\overrightarrow{e})}$$

A nonzero value of A is clearly parity nonconserving.

At incident electron energies of 19.4 and 22.2 GeV, $<7^{2}$-1.6GeV^{2}, and $y=(E_{e^-in}$-^-out)/$E_{e^-in}=0.2l_{9}$ a significant asymmetry was found

$$A/q^{2}=(-9.5\pm 1.6)\times 10^{-5}\ (\mathrm{GeV})^{-2}.$$

For a given polarization of the electrons injected into the SLAC accelerator, the longitudinal polarization of the electrons hitting the deuterium target varied with E_{e}~ because of the precession of the spin. The observed asymmetry as a function of E_{e^-9} *i.e.*, the electron polarization, shown in Fig. 11, has the

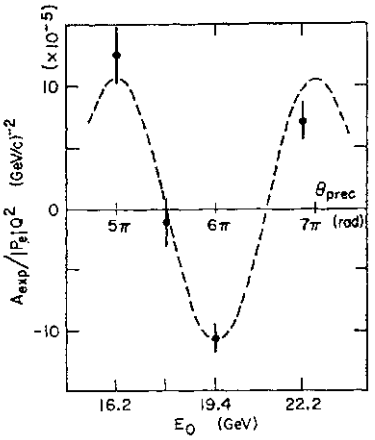

Fig. 11. Cross section asymmetry *vs* the electron beam energy in e~ (polarized)+d-»e~+. . . (from ref. 37).

correct behavior for a spin dependent asymmetry. This as well as many other careful consistency checks make the experiment very convincing.

The agreement between this result and the prediction of the W-S model for values of sin^{2} 6 determined by the neutrino experiments is very good, as shown on Fig. 12. The best value of the mixing angle from this experiment is

$$\sin^{2}\theta=0.20\pm 0.03.$$

This final conclusion is somewhat dependent

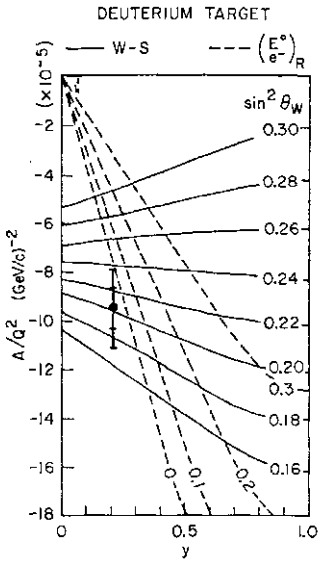

Fig. 12. Comparison of the experimental cross section asymmetry with the prediction of the W–S model for various values of sin^{2} θ (from ref. 37).

on quark-parton model assumptions. However, the uncertainties introduced by these assumptions are not very significant.

B. Determination of the neutral current couplings

In the previous section the experimental data were compared with the predictions of the W–S model. We saw that the data are consistent with these predictions. In this section we will discuss a "model independent" analysis in which no specific model is assumed at the outset. The experimental data will be used to determine the structure of the weak neutral currents in a general way. By structure of the weak neutral current we mean the space-time structure: vector (V), axial vector (A), scalar (S), pseudoscalar (P), or tensor (T) and the isotopic spin structure: isoscalar (I=0) or isovector (I=1). For the first time, at this conference, the experimental data are sufficient to produce a unique solution in a model independent analysis. As we will see, the resulting couplings are just those of the W–S model.

1. We start out by considering the general space-time structure.

(a) Any pure interaction (V, A, S, P, or T) must give the same neutrino and antineutrino cross sections for any given process. A difference in the ν and $\bar{\nu}$ cross section can only be caused by an interference between two different interactions with different C (like a VA

interference term). Experimentally, the results of the HPB experiment[38] for the elastic scattering process is

$$\frac{\sigma(\bar{\nu}_\mu + p \to \bar{\nu}_\mu + p)}{\sigma(\nu_\mu + p \to \nu_\mu + p)} = 0.53 \pm 0.17$$

and for the inelastic inclusive interactions the CDHS experiment[39] finds

$$\frac{\sigma(\bar{\nu}_\mu + N \to \bar{\nu}_\mu + \cdots)}{\sigma(\nu_\mu + N \to \nu_\mu + \cdots)} = 0.58 \pm 0.05.$$

These ratios are significantly different from unity so we can conclude that the neutral currents are not pure V, A, S, P or T.

(b) The distribution in $y=(E_{vin}-E_{vout})/E_{v\,in}$ for the inclusive neutral current process is sensitive to the space time structure of the interaction. For example,

$$\frac{d\sigma}{dy} \approx g(V-A) + g(V+A)(1-y)^2 + g(S, P)y^2$$

for ν scattering on real quarks. The y distributions for various interactions are shown in Fig. 13. Several experiments have looked at

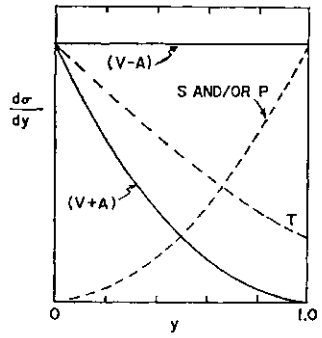

Fig. 13. Distributions in $y=(E_{in}-E_{out})/E_{in}$ for the process $\nu + N \to \nu + \ldots$ for various possibilities for the space-time structure of the neutral current interaction (neglecting antiquark contributions).

the y distribution of the inclusive neutral current reaction, using narrow band neutrino beams where the incident ν energy is known to some extent: the CITF experiment[40] at Fermilab, the CDHS experiment[41] at the CERN SPS, and the BEBC experiment[42] with a heavy neon fill at the CERN SPS. The conclusions are that:

i) S and/or P can be ruled out

$$\frac{g(V-A)+g(V+A)}{g(S, P)} = 0 \pm 0.03 \text{ BEBC}$$
$$= 0.02 \pm 0.07 \text{ CDHS}$$

(ii) Pure V, pure A, and pure (V+A) can be ruled out and pure (V—A) is unlikely

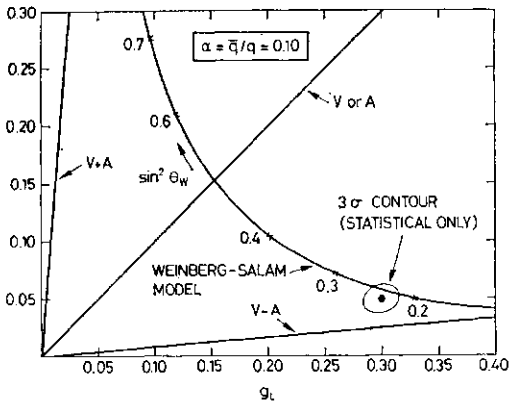

Fig. 14. Comparison of the experimental data for the V + A coupling (g_A) *vs* the V-A coupling (g_V) for various possibilities for the structure of the weak neutral current interaction (from ref. 41).

(see Fig. 14).

c) The parity violating asymmetry observed in polarized electron scattering at SLAC is due to an interference between the neutral currents and the electromagnetic interaction, which is a vector interaction. Thus the weak neutral current must have some V or A part to it.

2. In view of the above conclusions it seems reasonable to proceed with the analysis in terms of an arbitrary mixture of V and A interactions.

The various neutral current couplings between the leptons and the quarks are illustrated in Fig. 15. The purely leptonic processes, $\nu + e \to \nu + e$ depend only on the V and A couplings of the electron, g_V and g_A. In neutrino hadron scattering, isotopic spin is also relevant, so we have four couplings, V and A with *1=0* and *1=1* each. Sakurai[43] introduced the four couplings *a*, /3, *y* and *8* for (V, 7=1), (A, 7=1), (V, 7-0), and (A, 7=0), respectively. Sehgal[44] introduced an

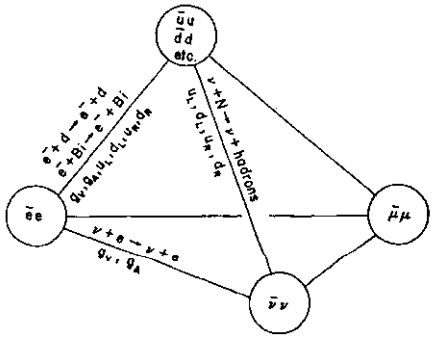

Fig. 15. Schematic diagram illustrating the various neutral current coupling constants (after ref. 43).

alternate four coupling constants u_L, d_L, u_R, and d_R. The subscript L and R are for (V—A) and (V+A) combinations, and the u and d are the isospin combination appropriate for the u and d quarks. The two sets of coupling constants are obviously just linear combinations of each other:

$$u_L = 1/4(\alpha+\beta+\gamma+\delta)$$
$$d_L = 1/4(-\alpha-\beta+\gamma+\delta)$$
$$u_R = 1/4(\alpha-\beta+\gamma-\delta)$$
$$d_R = 1/4(-\alpha+\beta+\gamma-\delta)$$

The parity violating effects in atomic bismuth or polarized electron scattering depend on six coupling constants: g_{A9} g_v for the electrons, and u_L, d_{L9} u_{R9} and d_R for the quarks. At this point some theoretical assumptions have crept in. The fact that g_A, g_v for the last case are the same as g_{A9} g_v for v+e-»v+e scattering depends on the assumption that the same Z° mediates both processes and that the neutrino couples to this Z° with the normal V-A coupling.

3. Determination of the v-quark couplings. The analysis follows the work of Sehgal,[44] Hung and Sakurai,[45] Abbott and Barnett,[46] Sidhu and Langacker,[47] Paschos,[48] and Claudson, Paschos and Sulak.[49]

(a) The neutral to charged current ratios for the inclusive channel are used to determine the overall strengths $(ui+dl)$ and $(u^2_R+d_R)$. These are the circular bands on the u_L *vs* d_L and the u_R *vs* d_R planes, shown in Fig. 16.

(b) The charge ratios in inclusive pion production select four allowed solutions A, B, C, and D indicated on Fig. 16. The data used comes from the Gargamelle experiment[50] at the CERN PS.

$$\frac{\nu+N\to\nu+\pi^++\cdots}{\nu+N\to\nu+\pi^-+\cdots}=0.77\pm0.14$$

$$\frac{\bar\nu+N\to\bar\nu+\pi^++\cdots}{\bar\nu+N\to\bar\nu+\pi^-+\cdots}=1.64\pm0.36.$$

(c) Recent results on the exclusive channels, v+p-»v+p from the HPB experiment[15] at Brookhaven and y + N - * y + N + 7 r from the Gargamelle propane experiment[21] at the CERN PS, select solution A as the only one allowed, as illustrated on Fig. 17.

The weakest part in this analysis is step (b), since the interpretation of the inclusive pion production data are quark-parton model dependent and the Gargamelle experiment was done at low neutrino energies. In a paper by Claudson, Paschos and Sulak[49] submitted to the Conference a similar analysis is carried out but the reliance on the inclusive pion ratios

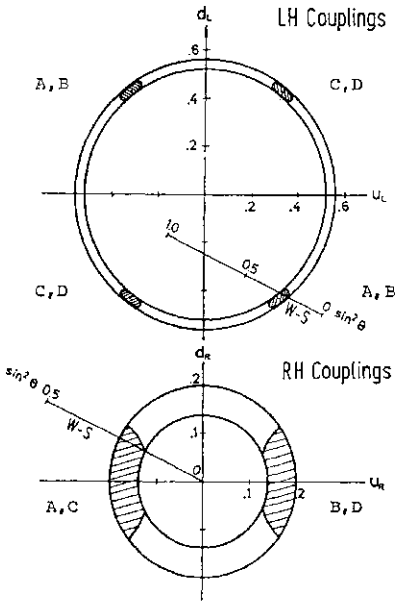

Fig. 16. Experimentally allowed values of the neutrino-quark neutral current coupling constants. A, B, C, and D indicate the solutions discussed in the text (from ref. 44).

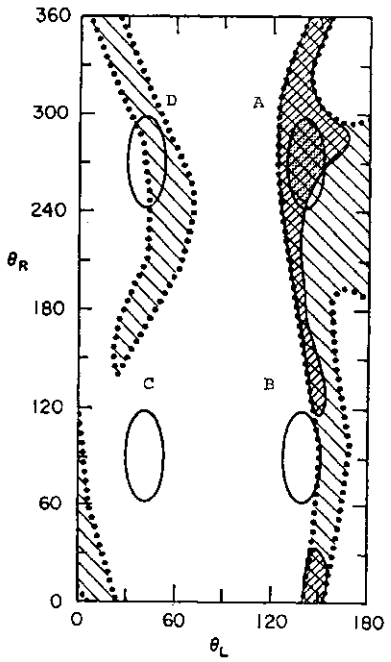

Fig. 17. The allowed angles in the L and R coupling planes of Fig. 16, with the solutions A, B, C, and D indicated. The shaded regions are those allowed by the elastic data. The doubly shaded region is that allowed by the single pion production data as well. Only solution A is consistent with all of the data (from ref. 46).

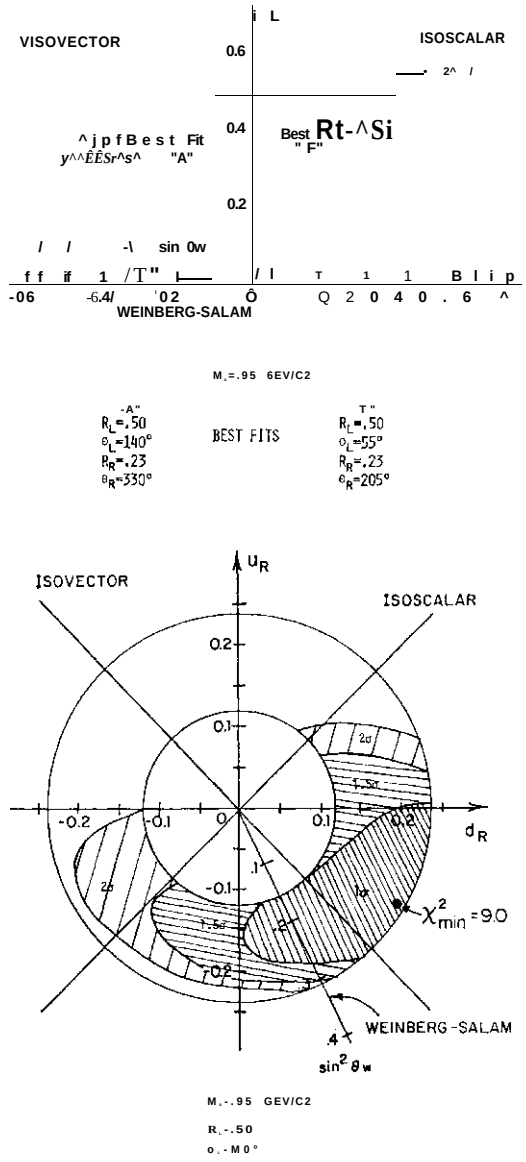

Fig. 18. Allowed regions in the u_L—d_L and the *UR—djt* coupling constant planes from the analysis of ref. 49.

is eliminated. The inclusive neutral current process is used to obtain *(u\+dl)* and (w|+</£), as above. The improved i^+p-n^+P and ï>+p-»iv+P data from the HPB experiment[15] is then used to obtain the solutions A and F shown on Fig. 18. Solution F, which is almost pure isoscalar, is ruled out using the fact that the J(1238) is produced in neutral current single pion production. This leaves solution A, which is essentially the same as solution A obtained by the analysis outlined above.

The values of the coupling constants for the unique solution are listed in Table VIII.

4. Determination of the v-electron couplings.

(a) The intersections of the regions allowed in the g_v-g_A plane by the cross sections for the processes, i^+e^-^+e⁻ and v_e+e~-+ £$_e$+e~ produces two ambiguous solutions, one with $gv \sim 0, g_A \sim -1/2$, the other with $g_v \sim -1/2$, $gv \sim 0$, as shown in Fig. 19. The region allowed by the cross section for i^«+e~ e~ is consistent with these two solutions but does not distinguish between them.

(b) The region in the g_v-g_A plane allowed by the parity violating asymmetry in polarized electron scattering observed at SLAC[37] is also shown on Fig. 19. This region overlaps the solution near $g_v \sim 0$, $g_A \sim -1/2$, but not the other solution and thus resolves the ambiguity. The values of g_v and g_A with errors for this solution are also listed in Table VIII.

Table VIII. Summary of the weak neutral current couplings.

Coupling constant	Value in Unique solution*	Weinberg-Salam	
		$\sin^2\theta = 1/4$	As Function of $\sin^2\theta$
g_V	0.0±0.1	0.0	-1/2+2sin²0
g_A	0.55±0.1	-0.5	-1/2
	0.35±0.07	0.33	1/2-2/3sin²0
d_L	~0.40±0.07	-0.42	-1/2+1/3sin²0
u_R	-0.19±0.06	-0.17	-2/3 $\sin^2\theta$
d_R	0.0 ±0.11	0.08	1/3 $\sin^2\theta$

* Using solution A of Abbott & Barnett.

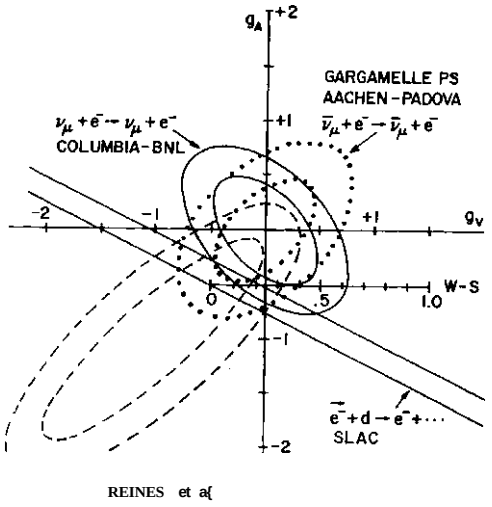

Fig. 19. Allowed regions in the neutrino-electron coupling plane, g_A *vs* g_v.

C. Summary of neutral currents

1. The "model independent" analysis now produces a unique solution. The values of the neutral current couplings for this solution are summarized in Table VIII. The

Table IX. Summary of neutral currents comparison with the Weinberg-Salam model.

Process	Experimental results	$\sin^2\theta$	W-S Prediction with $\sin^2\theta=0.23$
1. Purely leptonic			
$\nu_e+e^-\to\nu_e+e^-$	$(5.7\pm1.2)\times10^{-42}$ E$_\nu$ cm^2	0.29 ± 0.05	5.0
$\nu_\mu+e^-\to\nu_\mu+e^-$	$(1.7\pm0.5)\times10^{-42}$ E$_\nu$ cm^2	$0.21^{+0.08}_{-0.09}$	1.5
$\bar\nu_\mu+e^-\to\mu^-+\nu_e$	$(1.8\pm0.9)\times10^{-42}$ E$_{\bar\nu}$ cm^2	0.30 ± 0.18	1.3
2. Elastic scattering			
$\nu_\mu+p\to\nu_\mu+p$	(0.11 ± 0.02) $\times$ *form factor*	0.26 ± 0.06	0.12
$\bar\nu_\mu+p\to\bar\nu_\mu+p$	$(0.19\pm0.08)\times$ *form factor*	<0.5	0.11
3. Single pion production			
$\nu+N\to\nu+N+\pi^0$	(0.45 ± 0.08) $\times$ *(ν? ii ~ + N+ππ°)*	0.22 ± 0.09	0.42
$\nu_\mu+N\to\mu+N+\pi^+$	$(0.57\pm0.11)\times$ *(ν→+N→μ⁻+N+7r°)*	0.15-0.52	0.60
4. Inclusive			
$\nu/\bar\nu+N\to\nu+H$ ——	$(0.29\pm0.01)\times\nu+N$ *(ν/ν-H——)*	0.24 ± 0.02	0.30
$\nu+N\to\mu^-+H$ ——	(0.35 ± 0.025) $\times$ *aiPfi+N-+ + • • •)*	0.3 ± 0.1	0.38

couplings in the W-S model are also listed on the table. The agreement is very good with a value of $\sin^2\theta\sim1/4$.

2. The experimental results on the neutrino induced neutral current processes are summarized in Table IX. The agreement with the W-S model is excellent in all cases, as can be seen by comparing the second and fourth columns on the table.

3. The values of $\sin^2\theta$ obtained from each reaction are listed in the third column of Table IX. These values are displayed on Fig. 20. They are in very good agreement with each other. The weighted average for all of the reactions is

$$\sin^2\theta=0.23\pm0.02.$$

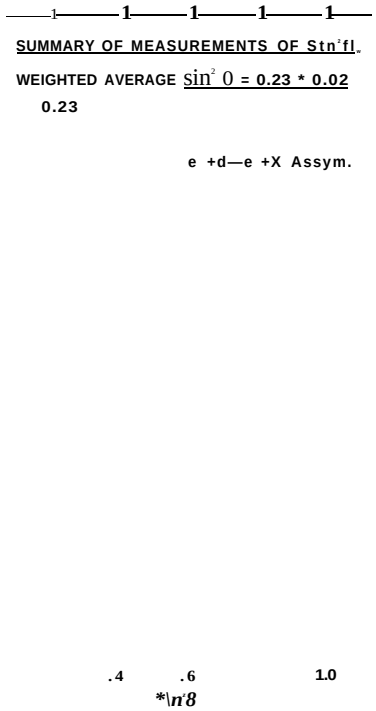

Fig. 20. Determination of the mixing angle, $\sin^2\theta$, from the various neutral current reactions.

§111. Charm Production by Neutrinos

The production of particles with the new hadronic quantum number, charm, has been observed in neutrino interactions both *via* the semileptonic and the hadronic decays of the charmed particles (C):

$$\nu+N\to\nu+C+\cdots$$

$$L\to\nu^-+\nu^+-\bullet\bullet \text{ or } e^-+\nu+-\bullet\bullet$$

$$\to K^0\pi^+\pi^-$$

The signature of the first process is the presence of two charged leptons in the final state: *i.e.*, dilepton events, like $\mu^-\mu^+$ or $\mu^-\pi^+$. The signature of the second process is a τ and a visible strange particle decay such as $K^0\to\pi^+\pi^-$ (vee) in the final state. In the first case there is an undetected ν in the final state so that the mass of the charmed particle cannot be reconstructed from its decay products. The evidence that these dilepton events come from charm production is the correlation of these events with strange particle production and the consistency of the rate and other properties of the events with the GIM scheme. In the case of the hadronic decays, all of the decay products are seen and the charmed particle can thus be directly observed as a peak in a mass distribution.

A. Dimuon production in counter experiments

Dimuon production by neutrinos has first been observed by the HPWF experiment[51] at

Table X. Dimuon production by and *î>p.* in the large counter experiments.

Experiment	ν_μ Induced		$\bar{\nu}_\mu$ Induced	
	Events*	$\mu^-\mu^+/\mu^-$	Events*	$\mu^+\mu^-/\mu^+$
HPWF[51] Fermilab	~160	0.4± 0.08%	~90	0.27± 0.09%
CITF[52] Fermilab	90	~1%	33	~1%
CHHS[53] CERN SPS	256	~1%	58	~1%

* The numbers listed are the number of events published. All three experiments have much larger samples from recent runs which are being analyzed.

Fermilab, soon followed by the CITF experiment[52] at Fermilab and later by the CDHS experiment[53] at the CERN SPS. The results of these three experiments on opposite sign dimuons ***(ju~ j u⁺)*** are summarized in Table X. Like sign dimuon production and trilepton production has been discussed in the previous talk by Professor Tittel. The rates for the *fi~/u⁻* events relative to single *pC* events are somewhat below 1 %, as shown in Figs. 21 and 22 for the HPW and the CDHS experiments, respectively. These rates seem to increase very rapidly with increasing E_ν. However, this effect is now understood to be caused by

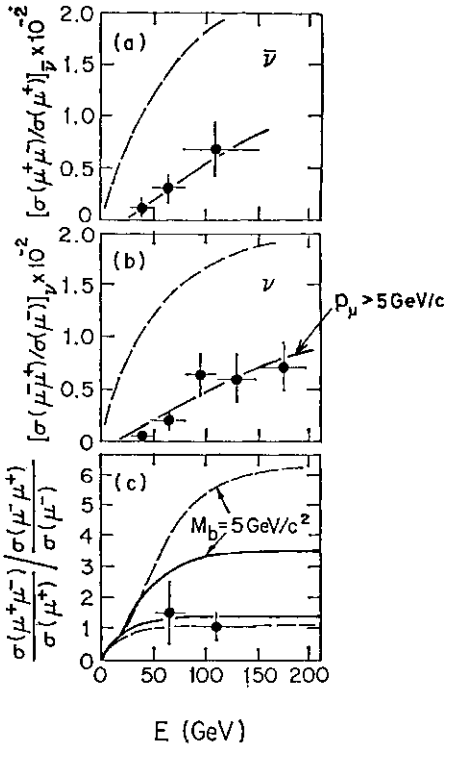

Fig. 21. The *ju~ ^⁺* production rate relative to the total charged current cross section in the HPWF experiment (from ref. 51).

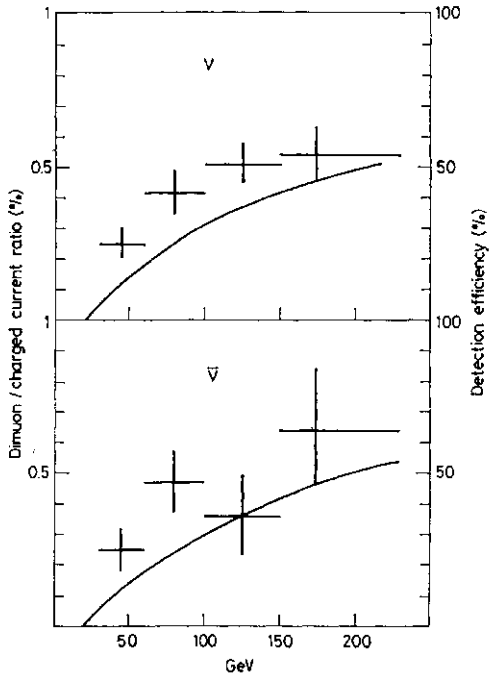

Fig. 22. The */u~fx⁻* production rate relative to the total charged current cross section in the CDHS experiment (from ref. 53).

the severe cuts (i%>4 or 4 1/2 GeV/c) imposed on the muon momenta in these experiments. The *x* and^ distributions for the dimuon events from the HPWF and the CDHS experiments are shown in Figs. 23 and 24, respectively.

B. Dilepton production in bubble chamber experiments

In the large bubble chambers filled with heavy liquids such as neon or freon the electron identification is very good and thus neutrino interactions, $\nu_{//}$+N->//~+e⁺+• • -,

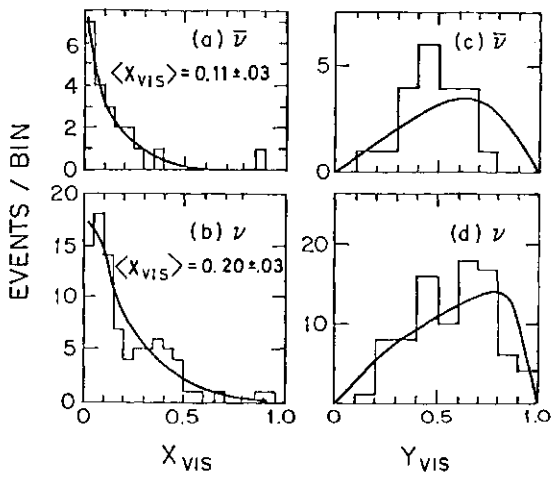

Fig. 23. Distribution in *x=q²/2mv* and *y=é/E* for the *ju~p⁻* events in the HPWF experiment (from ref. 51).

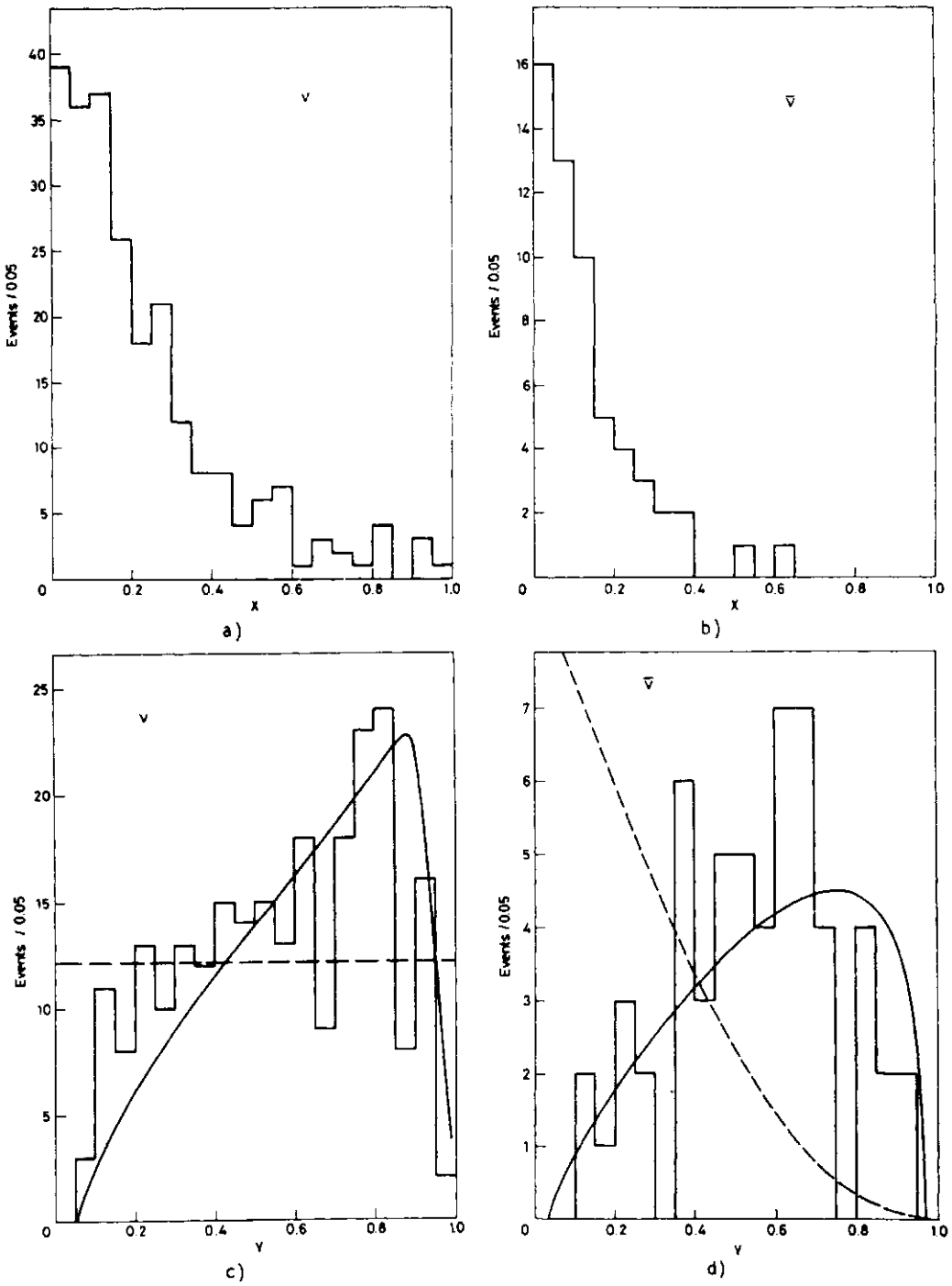

Fig. 24. Distribution in *x* and *y* for the \i *fi*⁺ events in the CDHS experiment (from ref. 53).

can be identified with very small backgrounds (typically 10-15%). Using external muon identifiers, production can also be isolated. The results of these experiments are summarized in Table XI for ν_μ experiments and in Table XII for experiments. In these experiments neutral strange particles can be detected *via* their decays K°-»7r⁺+7r" and *A*^-^*p*+*n*" (vees). The number of vees observed with these dilepton events is also listed on these tables. There is a significant correlation with strange particle production. For example in the Columbia-BNL experiment[56] the visible vee production in charged current (single ***JU~)*** events has been measured to be 6%. Thus ~15 vees would be expected with the 204 */**u*~*e*⁺ events, but 43 were observed.

In the selection of the */**u*~*e*⁺ events much less stringent cuts were imposed on the lepton momenta than in the counter experiments. For example in the Columbia-BNL experiment no cut was imposed on P_ν-, and a 300

Table XI. Dilepton production by neutrinos in bubble chambers.

Experiment	E_ν GeV	Liquid	Events Obs.	Vees Obs.	$\mu^- l^+/\mu^-$ Rate (%)
Gargamelle[54]	1–8	Freon	14	3	0.31 ± 0.13
CERN PS			μ^-e^+		
WISC–CERN–Hawaii–LBL[55]	~30	21% Ne	17	11	$0.8\ \pm0.3$
Fermilab E-28			μ^-e^+		
Columbia–Brookhaven[56]	~30	64% Ne	204	43	$0.5\ \pm0.15$
Fermilab E-53			μ^-e^+		
Berkeley–Seattle–LBL–Haw[57]	~30	64% Ne	6	1	$0.34^{+0.23}_{-0.18}$
Fermilab E-172			μ^-e^+		
Fermilab–LBL–Hawaii[58]	~50	50% Ne	9	1	
Fermilab E-460			$\mu^-\mu^+$		
BEBC Narrowband[59]	~75	60% Ne	5	2	$0.7\ \pm0.3$
CERN SPS			μ^-e^+		
BEBC Narrowband[60]	~75	60% Ne	11	6	$0.8\ \pm0.3$
CERN SPS			$\mu^-\mu^+$		
BEBC Wideband[61]	~30	60% Ne	17	6	0.41 ± 0.15
CERN SPS			μ^-e^+		
Fermi–Mich–IHEP–ITEP[62]	~30	64% Ne	6	1	$0\ \ \pm1/2$
Fermilab E-180			μ^-e^+		
F–W–B–LBL–S[63]	~50	45% Ne	40	5	0.54 ± 0.14
Fermilab E-546			$\mu^-\mu^+$		
Gargamelle[64]	~30	Freon	70	8	0.62 ± 0.18
CERN SPS			$\mu^-\mu^+$		
SKAT[65]	2–30	Freon	3	1	$0.7\ \pm0.4$
Serpukhov			μ^-e^+		
Totals			402	88	$0.5\ \pm0.1$

Table XII. Dilepton production by antineutrinos in the 15 ft bubble chamber.

Experiment	Liquid	Pictures	μ^+e^- Events	Background	Rae μ^+e^-/μ^+	Vees
Fermilab–Serpukhov–Moscow–Michigan[66] E-180	21% Ne	74,000	— 1	0.2 ± 0.2	$\leq0.5\%$	
Berkeley–Hawaii–Seattle[67] E-172	64% Ne	59,000	4	0.6	$0.15^{+0.14}_{-0.08}$	2
Fermilab–Serpukhov–Moscow–Michigan[68] E-180	64% Ne	~150,000	12	—2	$0.22\pm0.07\%$	7
Total			16		0.20 ± 0.06	9

MeV/c cut was imposed on P_e+. Thus essentially the whole signal is observed, as shown in Fig. 25. The cuts used by the counter experiments throw out most of the signal, especially at low E_ν. The rates observed for the dilepton events relative to single *li* events in the bubble chamber experiments are consistent with each other. The weighted average rate is (0.5±0.1)% for neutrinos and (0.20±0.06)% for antineutrinos. The energy dependence of the cross section for the *jbt~e*⁺ events, shown in Fig. 26, seems relatively constant or possibly rising gently relative to the total charged current cross section in this energy range. The sharp rise observed by the counter experiments can be understood as an effect of the selection cuts on the muon momenta. For example, if the same cuts, *Pfi,,>4.5* GeV/c, are applied to the *JU~q*⁺ events of the Columbia-BNL experiment, the rate is found to rise with E_ν as shown in Fig. 27. For comparison the rates measured in the CDHS experiment for *pr JU*⁺ events is also shown on this figure. The agreement is very good, indicating that the //~e⁺ and the *jLt~fi*⁺ events have the same origin.

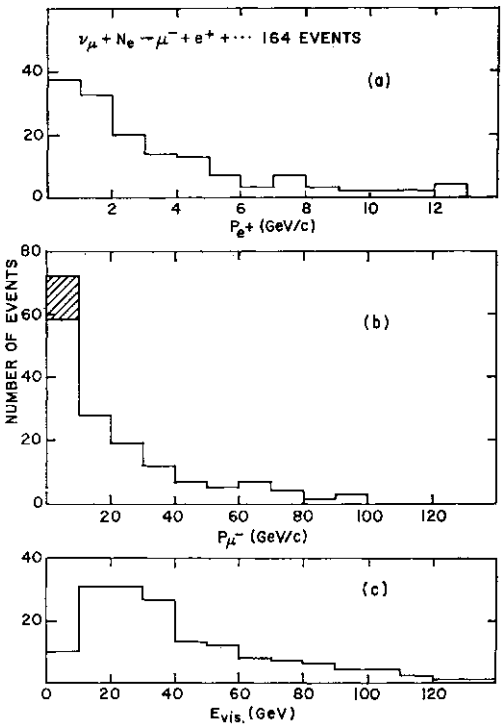

Fig. 25. Distributions in a) the positron momentum P_{e^+}, b) the muon momentum P_{μ^-} and c) the total visible energy E_{vis} for the $\nu_\mu e^+$ events in the Columbia-BNL experiment (from ref. 78).

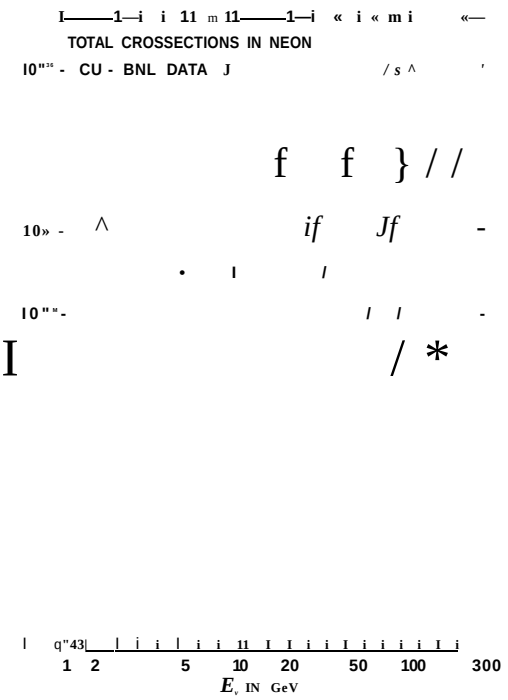

Fig. 26. Production cross section as a function of incoming neutrino energy E_ν for the $\nu_\mu e^+$ events relative to other neutrino interaction cross sections. The data points are from the Columbia-BNL experiment.

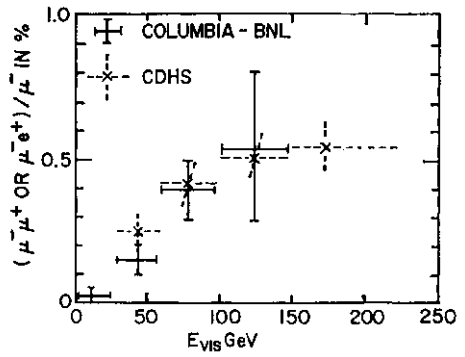

Fig. 27. Comparison of the relative production rates of the ν_μ and the $\nu_\mu/\bar{\nu}_\mu$ events using the same $E_\nu > 4.5$ GeV/c cut on both samples.

C. *Evidence that dilepton production is related to charm*

The observed dilepton events are not consistent with being single p^- events with the second lepton, the μ^+, or e^+, coming from π or K decay. The cross section for the dilepton events is too high by a factor of 10^3 to be due to the four fermion process $\nu pC/\mu^- \nu p$ or $\nu p \to \mu^- \nu_e$ in the Coulomb field of the target nucleus. These events, therefore, must be due to some new effect, such as the production and decay of a heavy lepton, an intermediate boson, or charmed particles. The interpretation as heavy lepton production followed by decay into $\mu^- \nu \bar{\nu}$ or $\mu^- \nu e^+$ was ruled out by the observation that the p^- carried much more energy on the average than the μ^+ or e^+ (see Fig. 25), which is not what is expected for heavy lepton decay as pointed out by Pais and Treiman.[69] The interpretation as production and decay of an intermediate boson is inconsistent with the energy dependence of the cross section (see Fig. 26) and the high inelasticity of the dilepton events. The interpretation of these events as the production and semileptonic decay of charmed particles is consistent with all aspects of the data, as will now be discussed in more detail.

1. The rate of 1/2 to 1% of the total charged current cross section, with a semileptonic branching ratio around 1/10, indicates 5 to 10% charm production as expected from $\sin^2 \theta_c$.

2. The x and y distributions are consistent with the dominant charm production mechanisms:

i. For incident :

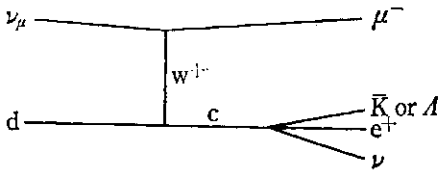

On valence quarks: Rate $\sim d(x) \sin^2 \theta_c$ 1 strange particle/event broad x distribution

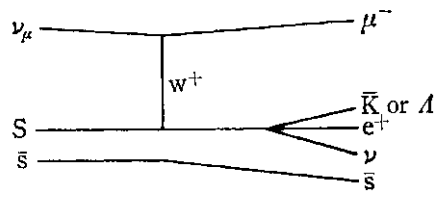

On sea quarks: Rate $\sim s(x) \cos^2 \theta_c$ 2 strange particles/event narrow x distribution

ii. For incident i^ , charm can be produced on sea quarks :

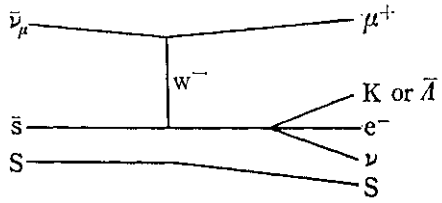

On s sea quarks: Rate $\sim s(x) \cos^2 \theta_c$ 2 strange particles/event narrow x distribution

We thus expect the x distribution for i^+N-* *fi~+I-*——to be a combination of the valence and sea x distribution, while for i^+N-*^"'+/"H——to be narrow like the sea x distribution, as observed (see Figs. 23 and 24). For example in the Columbia-BNL experiment, a fit to the x distribution to (1) (sea)+(l — a)(valence) produced a good fit with tf=0.37±0.10 (see Fig. 28) implying that charm production occurs about 1/3 of the time off sea s quarks and 2/3 of the time off valence quarks. Similar analyses, as well as the $\nu/\bar{\nu}$ ratio for dilepton production, lead to the following estimates of the fraction of s or $\bar{s}$ quarks relative to valence d quarks:

s or $\bar{s}$ (sea)
valence d quarks
=(3±2)% Columbia-BNL, x distribution
=(5±2)% CDHS, $\nu/\bar{\nu}$ ratio
=(9.9±3.5)% HPWF, x distribution
=(6.6±6A)% HPWF, $\nu/\bar{\nu}$ ratio.

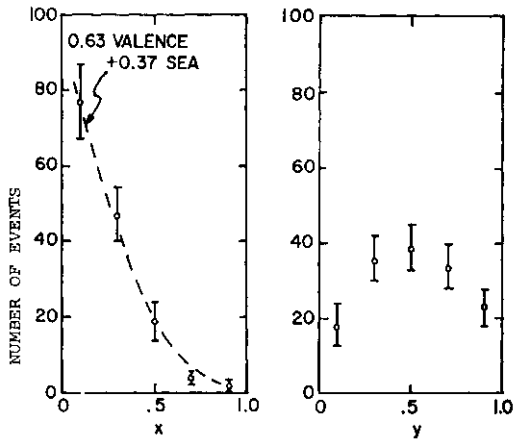

Fig. 28. Distributions in x and y for the ^~e$^+$ events of ref. 56. The curve is the best fit of a combination of valence and sea quark x distributions to the data.

3. Strange particle production. The visible vee production (K°->;r+7r~ and *A-*pn~)* in the dilepton events (see Table XI) is:

43 vees in 204 events—Columbia-BNL
45 vees in 198 events—all others combined
88 vees in 402 events—Total;

or, ~21 % visible vee production. Correcting for decay branching ratios, detection efficiencies, etc. Columbia-BNL obtain a rate of 0.6±0.1 total neutral strange particle production per *JU~Q-* event. If the number of charged strange particles equal the number of neutral strange particles produced in these events, this rate leads to a total of

~ 1.2 strange particles/event.

This agrees well with what we would expect from the G-I-M scheme, keeping in mind that from the fit to the x distribution we have 2/3 of the events on valence quarks with 1 strange particle per event plus 1/3 on sea quarks with 2 strange particles per event for a total expectation of 1 1/3 strange particles per event.

4. The detailed distributions of the dilepton events, such as the aximuthal angular distributions of the transverse momenta of the the p^+ or e$^+$, and the hadrons, the distributions in P and $P_\pm$ of the leptons, and the total hadronic energies, etc. are all in good agreement with what is expected from charm production. The K°e$^+$ mass distribution from the !^+Ne-»//~+e$^+$+K°H——events, shown in Fig. 29, is in good agreement with the semileptonic decay of a D meson.

D. *Direct observation of charm production via the hadronic decays* $D^0 \to K^0 \pi^+ \pi^-$

In the Columbia-BNL exneriment[70] usine

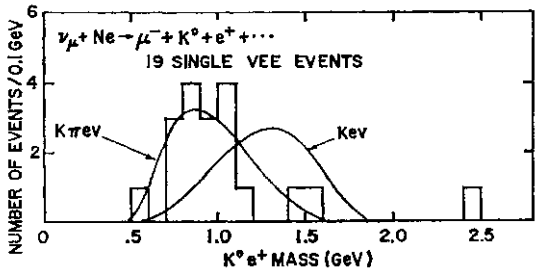

Fig. 29. Distribution in the K°e⁺ effective mass from the reaction j^+Ne->Ai~+e⁺+K°H——in the Columbia-BNL experiment.

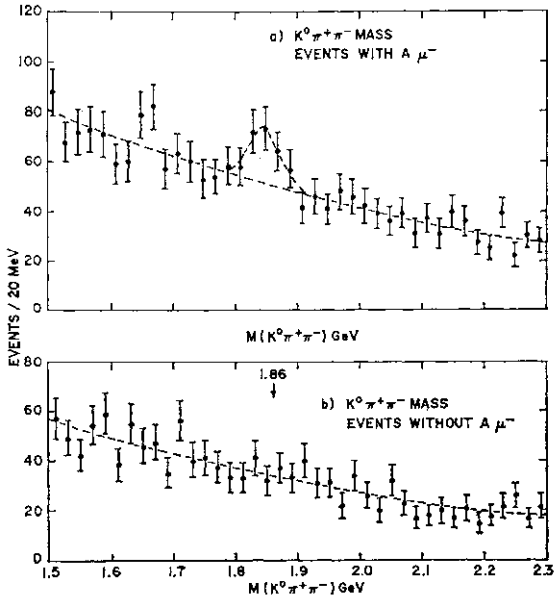

Fig. 30. Distribution in the K°+7r⁺+7r- effective mass in the reaction ^+Ne^//"+K°+TT⁺+7T"+ ... in the Columbia-BNL experiment (from ref. 70).

a heavy neonhydrogen mix in the Fermilab 15 ft chamber, a total of 1815 i^+Ne->/r+K°H——and 1367 z^+Ne->^-+/l°+••• events have been measured. A peak in the K°7r⁺7r~ mass distribution is observed at the mass of the D° discovered at SLAC, as shown in Fig. 30a. The signal is ~60 events above background, with a statistical significance of four standard deviations. The mass and width of this peak are:

$$m = 1850 \pm 15\ \text{MeV}$$

$$< 7 > = 20 \pm 10\ \text{MeV}.$$

The observed width is consistent with the mass resolution of the experiment as expected for a very short-lived particle. No corresponding peak is observed in events without a *ju~* in the final state (Fig. 30b) consistent with the prediction of the G-I-M scheme that charm changing neutral currents are absent. This effect is thus interpreted as the production and decay of a charmed D meson:

$$\nu_\mu + \text{Ne} \to \mu^- + \text{D}^0 + \cdots$$
$$\qquad\qquad\quad \lfloor \to \text{K}^0 + \pi^+ + \pi^-.$$

Correcting for K° branching ratios and detection efficiencies, this effect corresponds to a D°^K°7T⁺7r- decay in (0.7±0.2)% of all charged current *Vp.* interactions. The distribution in $Z = E_D o l E_{hai ATOnic}$, the charm fragmentation function, from this sample is shown in Fig. 31.

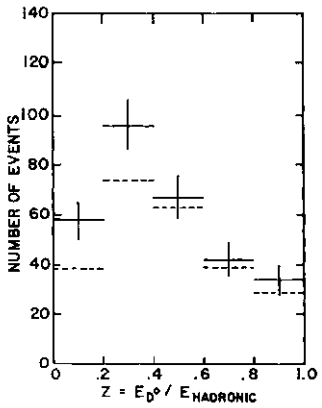

Fig. 31. Distribution in $Z = E_D o / E_{hdaTOnic}$ for the p_AI+Ne->A*"+D°+ ..D°->K°7r⁺7r events in the Columbia-BNL experiment (from ref. 70).

E. Limits on charm changing neutral currents

Charm changing neutral current interactions were looked for both in production and decay processes.

1. Charm production by neutrinos via neutral currents would lead to

$$\nu_\mu + \text{N} \to \nu_\mu + \text{C} + \cdots$$
$$\qquad\qquad\quad \lfloor \to e^+ + \nu_e + \text{hadrons}$$
$$\qquad\qquad\quad \lfloor \to \mu^+ + \nu_\mu + \text{hadrons}.$$

The signature for this process would be events with an e⁺ or *j u*⁺ in the final state but no */u~.* Such a search has been carried out in the Columbia-BNL[71] and the Fermilab-Michigan-IHEP-ITEP experiments[72] at Fermilab looking for e⁺, and in the CDHS experiment[73] at CERN looking for //⁺, all with negative results. The best limit was obtained in the CDHS experiment

$$\frac{\sigma(\text{charm changing neutral currents})}{\sigma(\text{total neutral currents})} \leq 2.6\%.$$

2. Charm changing neutral currents would lead to decays of the type C->e⁺ + e~ + hadrons in analogy with the charm changing charged current decays, C-»e⁺+ν_e+hadrons. The Columbia-BNL experiment has carried out a search for such decays in the process:

$$\nu_\mu + N \rightarrow \mu^- C + \cdots \quad \big\lfloor \rightarrow e^+ + e^- + \text{hadrons},$$

where the signature is a ^~+e⁺+e~-l———in the final state. No signal was found, and an upper limit was set, using the 204 //~e⁺ events as normalization, of

$$\frac{\text{Rate (charm changing neutral currents)}}{\text{Rate (charm chaing charged currents)}} \leq 2\%.$$

§IV. Limits on Heavy Lepton Production

Searches for heavy lepton production by neutrinos have been carried out *via* their decays into electrons or //~+TT⁺, which will be discussed here. The search for heavy leptons in the tri-muon events observed in the counter experiments has been discussed by Professor Tittel in the previous talk.

A. Charged heavy leptons

Charged heavy leptons L* could be seen in neutrino interactions *via* the production and decay processes

$$\nu_\mu + N^\pm \rightarrow L + \text{hadrons} \quad \big\lfloor \rightarrow e^\pm + \nu + \bar{\nu} \quad \big\lfloor \rightarrow \mu^\pm + \nu + \bar{\nu}.$$

1. A search for L* using this reaction, looking for events with a single e* but no ***p T,*** was carried out by the Columbia-BNL experiment[74] with negative results. Their conclusions are:

(a) Muon type heavy leptons, if they exist, are heavier than:

$$m(L^-) \geq 7.5 \text{ GeV}$$
$$m(L^+) \geq 9.0 \text{ GeV}.$$

(b) The heavy lepton, r (1.8), discovered at SLAC is *not* muonlike.

(c) Any ***JU-T*** mixing is less than 2 1/2%.

2. Similar searches were carried out by the counter experiments by the CITF[75] and the CDHS[76] groups looking for events with a single ***/LC***⁺ but no with negative results. The best limit on the mass of a muon-type heavy lepton comes from the CDHS experiment

$$m(L^+) \geq 12 \text{ GeV}.$$

No limit is available from these experiments on m(L~) since a single ***ju~*** signature from L~ decay cannot be distinguished from the dominant charged current ν_μ interactions.

B. Neutral heavy leptons

Several experiments have found evidence suggestive of neutral heavy lepton production by neutrinos. These effects, however, have not been confirmed in other experiments.

1. The Aachen-Padova experiment[77] has reported 7.2:t3.7 events of the type i^+N-* //~+e⁺H———which they feel are not from charm production but might be due to heavy lepton decays. The rate for this effect is (1 to 3)x 10~⁴ depending on the E_u cut. This is at the CERN PS with incident neutrino energies of a few GeV.

The Columbia-BNL experiment[78] sees no evidence for such an effect. After cuts to separate L° production from charm production in the *pt~e*⁺ events (the effects of these cuts are model dependent) set a limit of < 2 x 10~⁴ on "non-charmlike" ***/u~c***⁺ events that could come from heavy lepton decays. This is at Fermilab energies where the cross section for the production of a light L° would be expected to be much higher than at the energies of the Aachen-Padova experiment.

2. A heavy liquid bubble chamber experiment[79] at SKAT at Serpukhov has reported 1 or 2 events of the type i^+N-^~+e⁺+••• where the ***ju~*** and the e⁺ originate from a common point which is not the neutrino interaction point *(i.e.,* there is a gap between the *v* interaction point and the beginning of the ***ju~*** and the e⁺ tracks). The possibility that these events might be due to the decay of a neutral heavy lepton has been suggested. These events are seen in a sample of ~500 charged current neutrino interactions.

The Columbia-BNL experiment[56] has observed *no* such events in a sample of ~80,000 charged current neutrino interactions.

3. Two experiments[80] in BEBC at the CERN SPS have presented evidence at the Oxford Neutrino Conference earlier this summer for a peak in the ^~7 r⁺ mass distribution

near 1.85 GeV in events of the type i^+N-* /z~+TT'H———. In a similar sample of events, applying the idential selection criteria as used in the BEBC experiment, the Columbia-BNL experiment[56] at Fermilab sees no such effect with comparable statistics. The effect is also not seen in the BFHSW experiment[81] E-546 in the Fermilab 15 ft chamber. Two other experiments, the BHS (Expt. 172)[82] and the FIIM (Expt. 45)[83] in the Fermilab 15 ft chamber have data relevant to this question. At this conference the BEBC experiment (talk by D.R.O. Morrison) reported that the transverse momentum distribution of the *TC*⁺ from the events in the */U~K*⁻ peak makes the interpretation of this effect as the decay of a heavy lepton unlikely.

In summary then, there appears to be no convincing evidence for either charged or neutral heavy lepton production in neutrino interactions.

References

1. F.J. Hasert *et al* (Gargamelle PS): Phys. Letters **46B** (1973) 138; A. Benvenuti *et al* (HPWF): Phys. Rev. Letters **32** (1974) 800; B. C. Barish *et al* (CITF): Phys. Rev. Letters **34** (1975) 538.
2. S. J. Barish *et al* (Argonne): Phys. Rev. Letters **33** (1974) 448; W. Lee *et al* (CIR): Phys. Rev. Letters **38** (1977) 202.
3. S. Weinberg: Phys. Rev. Letters **19** (1967) 1264; A. Salam: in ***Elementary Particle Theory,*** ed. by N. Svartholm (Stockholm 1968), p. 367.
4. S. L. Glashow, J. Iliopoulos and L. Maiani: Phys. Rev. **D2** (1970) 1285.
5. F. Reines *et al:* Phys. Rev. Letters **37** (1976) 315.
6. J. Blietschau *et al:* Phys. Letters **73B** (1978) 232.
7. H. Faissner *et al:* Phys. Rev. Letters **41** (1978) 213.
8. P. Alibran *et al :* Phys. Letters **74B** (1978) 422. M. Haguenauer: talk B6-5 at this Conference, and private communication.
9. A. M. Cnops *et al :* Phys. Rev. Letters **41** (1978) 357.
10. J. Blietschau *et al :* Nucl. Phys. **B114** (1976) 189.
11. H. Faissner *et al:* Phys. Rev. Letters **41** (1978) 213.
12. R. Armenise *et al:* Paper submitted to the Oxford Conference on Neutrino Physics, Oxford University (1978).
13. B. Roe *et al:* Paper submitted to the Oxford Conference on Neutrino Physics, Oxford Uniniversity (1978).
14. M. Haguenauer: Talk no. B6-5 presented at this Conference.
15. H. H. Williams *et al:* Talk no. B5-3 presented at this Conference.
16. P. Sokolsky *et al:* Paper submitted to the Oxford Conference on Neutrino Physics, Oxford University (1978).
17. E. Radermacher: Talk no. B5-2 persented at this Conference.
18. M. Pohl *et al:* Phys. Letters **72B** (1978) 488.
19. W. Lee *et al* (CIR): Phys. Rev. Letters **38** (1977) 202; T. Hansl *et al* (Aachen-Padova): ***Proc. Int. Neutrino Conf.*** (Aachen, 1976), p. 278; F. **J.** Hasert *et al* (Gargamelle); Phys. Letters **59B** (1975) 485.
20. S. J. Barish *et al:* Phys. Rev. Letters **33** (1974) 448.
21. W. Krenz *et al:* Nucl. Phys. **B135** (1978) 45; O. Erriques *et al:* Phys. Letters **73B** (1978) 350.
22. S. L. Adler, S. Nussinov and E. Paschos: Phys. Rev. **D9** (1974) 2125; E. H. Monsay: Argonne Rpt. ANL-HEP-PR-78-08 (1978); L. E. Abbott and R. M. Barnett: SLAC-PUB-2136 (1978).
23. S. L. Adler: Ann. Phys. **50** (1968) 189; see also ref. 22.
24. J. Blietschau *et al :* Nucl. Phys. **B118** (1977) 218.
25. P. Wanderer *et al:* HPWF-77/1 (to be publ. in Phys. Rev.).
26. F. S. Merritt *et al :* CALT 68-627 (to be pubL in Phys. Rev.).
27. M. Holder *et al:* Phys. Letters **71B** (1977) 222; Phys. Letters **72B** (1977) 254.
28. E. Cazzoli *et al :* Brookhaven Preprint NG-301.
29. P.C. Bosetti *et al:* Phys. Letters **76B** (1978) 505.
30. J. Marriner: Ph.D. Thesis, LBL Rpt. LBL-6438 (1977).
31. E. A. Paschos and L. Wolfenstein: Phys. Rev. **D7** (1973) 91.
32. P.C. Bosetti *et al:* Phys. Letters **76B** (1978) 505.
33. N. Fortson: Proceedings of Neutrinos 78, Purdue U. (1978).
34. P. G. H. Sandars: Recent result presented at the RIGA Conference (1978).
35. L. M. Barkov *et al:* Pisma Zh. Eksp. Fiz. (JETP Letters) **26** (1978 379.
36. M. W. S. M. Brimicombe, C. E. Loving and P. G. H. Sandars: J. Phys. B. L. (1976) 237; E. M. Henley and L. Wilets: Phys. Rev. **A14** (1976) 1411; LB. Kriplovich: JETP Letters **20** (1974) 315.
37. C. Y. Prescott *et al:* Phys. Letters **77B** (1978) 347.
38. See ref. 15.
39. See ref. 27.
40. F. S. Merritt *et al*: Preprint CALT-68-600 (1977) 601.
41. M. Holder *et al :* Phys. Letters **72B** (1977) 254.
42. Aachen-Bonn-CERN-LONDON-Oxord-Saclay Collaboration: paper no. 965, sumbitted to this Conference.

43. J. J. Sakurai: Invited paper presented at Neutrino-77, Elbrus, USSR, June 1977.
44. L. M. Sehgal: Phys. Letters **71B** (1977) 99.
45. P. Q. Hung and J. J. Sakurai: Phys. Letters **72B** (1977) 208.
46. L. F. Abbott and R. M. Barnett: Phys. Rev. Letters **40** (1978) 1303; SLAC Preprint SLAC-PUB-2136 (1978).
47. P. Langacker, D. P. Sidhu, Phys. Letters **74B** (1978) 233; Phys. Rev. Letters **41** (1978) 732.
48. E. A. Paschos, Brookhaven National Laboratory, preprint no. BNL-24619 (1978).
49. M. Claudson, E. A. Paschos and L. R. Sulak: Paper no. 1158 submitted to this Conference.
50. H. Klutting, J. G. Morfin and W. van Doninck: Phys. Letters **71B** (1977) 446.
51. A. Benvenuti *et al :* Phys. Rev. Letters **34** (1975) 419; A. K. Mann: Talk no. B5-5, at this Conference.
52. B. C. Barish *et al.:* Phys. Rev. Letters **36** (1976) 939.
53. M. Holder *et al:* Phys. Letters **69B** (1977) 377.
54. J. Blietschau *et al:* Phys. Letters **60B** (1976) 207; H. Deden *et al:* Phys. Letters **67B** (1977) 474.
55. P. Bosetti *et al:* Phys. Rev. Letters **38** (1977) 1248.
56. C. Baltay *et al:* Phys. Rev. Letters **39** (1977) 62; R. B. Palmer *et al:* Talk no. B6-2 at this Conference.
57. H. C. Ballagh *et al :* Phys. Rev. Letters **39** (1977) 1650.
58. C. T. Murphy *et al : Proc. XIIth Rencontre de Moriond* (1977), p. 301.
59. P. Bosetti *et al:* Phys. Letters **73B** (1978) 380.
60. Same as ref. 59.
61. O. Erriques *et al:* Phys. Letters **77B** (1978) 227.
62. V. Ammosov *et al :* Paper no. 907 submitted to this Conference.
63. V. Z. Peterson *et al:* Paper no. 1122 submitted to this Conference.
64. M. Haguenauer: Talk no. B6-5 at this Conference.
65. D. S. Baranov *et al :* Paper no. 942 presented at this Conference.
66. J. P. Berge *et al:* Phys. Rev. Letters **38** (1977) 266.
67. H. C. Ballagh *et al:* Phys. Rev. Letters **39** (1977) 1650.
68. V. Ammosov *et al:* Paper no. 907 submitted to this Conference.
69. A. Pais, S. B. Trieiman: Phys. Rev. Letters **35** (1975) 1206.
70. C. Baltay *et al:* Phys. Rev. Letters **41** (1978) 73.
71. C. Baltary *et al : Proc. Neutrino 78 Conf,* Purdue University (1978).
72. V. Ammosov *et al:* Paper no. 921 submitted to this Conference.
73. M. Holder *et al:* Phys. Letters **74B** (1978) 277.
74. A. M. Cnops *et al* : Phys. Rev. Letters **40** (1978) 144.
75. B. C. Barish *et al:* Phys. Rev. Letters **32** (1974) 1387.
76. M. Holder *et al:* Phys. Letters **74B** (1978) 277.
77. E. Radermacher: Talk 5B-2 at this Conference.
78. C. Baltay *et al : Proc. Neutrino 78 Conf.,* Purdue University (1978).
79. D. S. Baranov *et al:* Phys. Letters **70B** (1977) 269; paper no. 942 at this Conference.
80. P. C Bosetti *et al : Proc. Oxford Neutrino Conf,* Oxford University (1978).
81. V. Z. Peterson: Private communication.
82. H. Lubatti: Private communication.
83. B. Roe: Private communication.

P8: Theory of Weak Interactions and Models of Elementary Particles

Chairman: H. HARARI

Speaker: S. WEINBERG

Scientific Secretaries: K. FUJIKAWA
Y. CHIKASHIGE

(Wednesday, August 30, 1978; 9: 00-10: 00)